Effects of liquid properties on the dynamics of under-liquid laser-induced shock process

Thao Thi Phuong Nguyen[1,2] · Rie Tanabe[2] · Yoshiro Ito[2]

Abstract We compared the shock processes induced when focusing a single laser pulse (1064 nm, FWHM = 13 ns) onto the surface of epoxy resin blocks immersed in glycerol, water, liquid paraffin, and silicone oils. A custom-designed time-resolved photoelasticity imaging technique was applied to observe the strength of stress wave induced inside the solid target and the propagation of shock waves in the liquid with time resolution of nanoseconds. We demonstrated that the shock impedance of the liquid caused a noticeable effect on the strength of laser-induced stress wave: Ablation in the liquid with a higher shock impedance resulted in a stronger stress. By using glycerol instead of water as the confining medium, the pulse energy required to induce a certain level of stress was reduced by about 20 %. The dynamical behaviors of the main shock wave and the reflected wave in inverted V-shape in each liquid are also discussed in details.

1 Introduction

When a laser pulse is focused on a solid–liquid interface, it vaporizes the material to create a high-pressure plasma, which induces a strong shock during its expansion. The liquid phase acts as the confining medium to restrict the expansion of the plasma and thus enhances the shock pressure. In most applications involving under-liquid laser-induced shock process (LSP), water is used as the confining medium [1–6]. However, a wide range of organic liquids has also been used in surface patterning, surface coating, and nanoparticle synthesis [6–9]. Several workers have observed the dynamics of LSP in water, but the studies aiming at the dynamics of LSP in other liquids have been rarely carried out. Burakov et al. [9] showed spectroscopic diagnostics of the laser-induced plasma on a metallic target in acetone, ethanol, and distilled water. But the dynamics of shock wave fronts have yet to be discussed in their report. O'Malley et al. [10] observed the laser-induced shock propagation in acetone and toluene when focusing a laser pulse on the liquid surface. The dynamics of laser-induced breakdown and shock waves in four alcohols were also reported in [11]. Yet, very little is known about the dynamical characteristics of shock process induced at the solid–liquid interface when organic liquids are used as the confining medium. A comparison of the shock process induced in various liquids will help expose the mechanism of under-liquid LSP further and is important when considering using another liquid instead of water as the confining medium for laser-induced ablation processes.

In our previous research, we observed the LSPs in glycerol, liquid paraffin and silicone oil at high intensities. The result showed that the impurities in organic liquids initiate breakdowns at multiple sites along the light path and significantly reduce the strength of the stress wave [12]. The study into the dynamical characteristics of LSPs in different liquids at fluences below breakdown threshold, however, has yet to be carried out. In this research, we chose low laser fluences to avoid the breakdowns induced in the liquid phase, on the solid–liquid interface as well as on the liquid–air interface. Under this experimental condition, we compared the shock processes induced in

✉ Yoshiro Ito
    itoy@vos.nagaokaut.ac.jp

1   Institute of Research and Development, Duy Tan University, K7/25 Quang Trung, Danang, Vietnam

2   Department of Mechanical Engineering, Nagaoka University of Technology, 1603-1 Kamitomioka, Nagaoka, Niigata 940-2188, Japan

glycerol, liquid paraffin, and silicone oils to that induced in water. The custom-designed time-resolved photoelasticity imaging technique was applied observe the strength of stress wave induced inside the solid and the propagation of shock waves into the liquid with time resolution of nanoseconds [12–14]. We report in this paper the discrepancies observed for the velocity of the shock wave, the angle of the reflected wave, and the strength of stress wave induced in LSPs in different liquids.

2 Experimental section

The experimental setup is similar to our previous reports [12–14], and only an outline is described here. The shock process was induced by focusing a single Q-switched Nd:YAG laser pulse (1064 nm, FWHM = 13 ns) by a 40-mm focal length lens onto a target surface. Targets were epoxy resin blocks of $25 \times 5.8 \times (18–20)$ mm^3 dimensions. The upper 25×5.8 mm^2 surface of the epoxy resin block was ground by sandpaper to obtain the roughness of 1.0 μm and was coated with black paint to enhance the shock process [13]. The target was placed in a glass cell filled with liquid. The target surface was located 4–5 mm under the liquid–air interface. Water, glycerol, liquid paraffin, and silicone oils were used as the liquid confining medium in our experiments. A Milli-Q ultrapure water system was used to provide ultrapure reagent-grade Type I water. Glycerol, liquid paraffin, and silicone oils were reagent grade and used as received. The ablation pulse energy was regulated in the range of 10–100 mJ, corresponding to the fluences of 5–50 J cm^{-2}. When focusing the laser light on the target surface, the distance between the lens and the target surface was adjusted to compensate for the effects of the different refractive indices of these liquids. A sheet of micro cover glass (~ 0.1 mm thick) was inserted between the lens and the target to protect the lens from ejecting substances.

The imaging system is a pump-and-probe system with polarizers and quarter-wave plates included to construct a circular polariscope in the bright field mode for capturing time-resolved photoelasticity images. The fundamental radiation (1064 nm) was used as the pump pulse (ablation pulse) and the second-harmonic radiation (532 nm) was used as the probe pulse. We defined the delay time as the interval between the rise of the pump pulse and the peak of the probe pulse. With this system, we can only capture one image for each ablation pulse. The measurements, therefore, needed to be repeated with various delay times between pump-and-probe pulses to observe the entire shock process. For delay times shorter than 100 ns, we used one laser source (Powerlite 8000) to generate both the pump-and-probe pulses. The delay time was provided by

passing the probe pulse through a variable optical delay line. For delay times from 100 to thousands of nanoseconds, we used the Powerlite 8000 to generate pump pulses and a second laser (NY 82) to generate probe pulses. The delay time between two pulses was provided by a delay generator.

3 Results and discussion

Figure 1a shows representative images of the shock process induced when focusing a 60 mJ laser pulse on targets immersed in water, glycerol, liquid paraffin, and silicone oil, observed in a short interval after the irradiation. At these early delay times, we can only observe a black area expanding on the target surface, which is the shadow of a shock wave traveling together with the gasified material [13]. The images show that there was no breakdown in the liquid phase, and the expansion of gasified material appeared to be the same for ablations in water and other liquids. Figure 1b shows the shock processes in the four liquids at 1500 ns. At this delay time, we can observe the main features involving in an under-liquid LSP: the main shock wave traveling into the liquid, the reflected waves in the inverted V-shape, the cavitation bubble, and the stress wave propagating into the solid target. The differences were observed for the slope of the V-shaped wave, the velocity of the shock wave, and the strength of the stress wave.

3.1 Slope of V-shaped wave

We measured the slopes of the V-shaped waves induced in water, liquid paraffin, and silicone oil at 1500 ns delay time. At this delay time, the waves already traveled a distance into the liquid phase, and the effect of high temperature of the plasma can be avoided. The slopes of the V-shaped waves were observed over the range of pulse energy from 10 to 100 mJ. The result showed that the slopes of the V-shaped waves had good stability in each liquid and were not dependent on laser pulse energy. These slopes were measured to be 34° (in water), 32.5° (in liquid paraffin), and 23° (in silicone oil) with the standard deviation of 0.5°. The V-shaped wave induced in glycerol dissipated after a few hundreds of nanoseconds and cannot be observed at 1500 ns. We, therefore, measured its slope at earlier delay times, around 400–500 ns. The measured value was 50° with the standard deviation of 1.5°.

The reflected waves in the inverted V-shape have been observed in underwater LSP [13–15] but have not been reported for other liquids. Our result demonstrated that these V-shaped waves can also be induced in laser ablation of material in organic liquids. Since the V-shaped wave
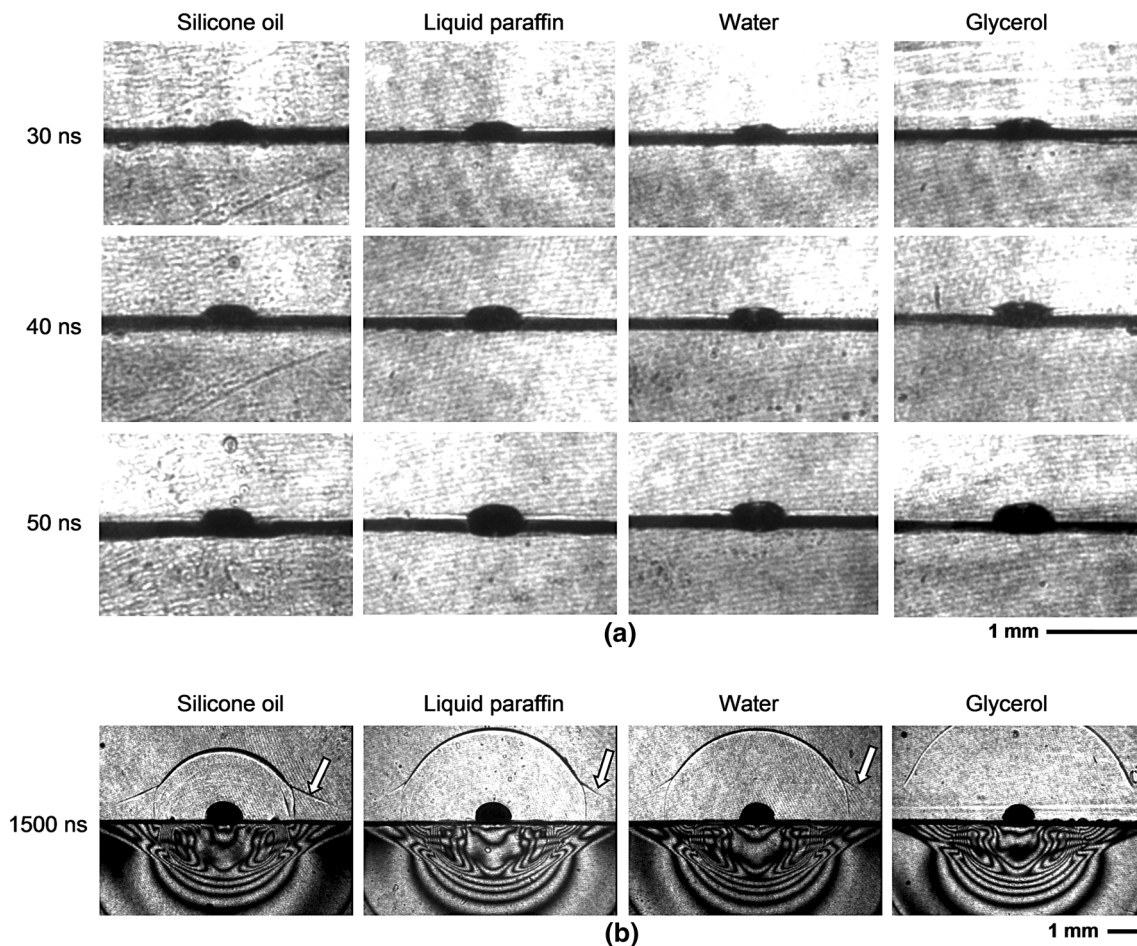
Fig. 1 Photoelasticity images of laser-induced shock process in water, glycerol, liquid paraffin, and silicone oil observed at **a** early delay times and **b** at 1500 ns after irradiation. The pulse energy was 60 mJ. The *arrows* point out the V-shaped waves induced in the liquids

was caused by the reflection of shock wave into the liquid when traveling along the solid–liquid interface [13], the discrepancies in the slopes of the V-shaped waves observed in our experiment can be explained by the difference in acoustic properties of these liquids. We used the slope α of the V-shaped wave to estimate the acoustic velocity in the liquids: $c_{liquid} = c_{solid} \sin \alpha$. Here we used the value of acoustic velocity in epoxy resin $c_{solid} = 2660 \pm 30$ m s^{-1}, as has been measured in our previous report [13]. The acoustic velocities calculated from the slopes of the V-shaped waves were 1490 ± 30 m s^{-1} (in water), 1430 ± 40 m s^{-1} (in liquid paraffin), and 1040 ± 30 m s^{-1} (in silicone oil). These values show good agreement with the published ones, which were 1482 m s^{-1} for water [16], 1420 m s^{-1} for liquid paraffin [17], and 1000 m s^{-1} for silicone oil [18]. The acoustic velocity calculated from the slope of the V-shaped wave for glycerol was 2040 ± 50 m s^{-1}. Compared to the published data for acoustic velocity in glycerol, which is 1920 m s^{-1} [17], the value measured in our experiment is higher. This difference can be explained by that the slope

of the V-shaped wave induced in glycerol was measured at the too early delay times, and thus the high temperature of the laser-induced plasma caused a noticeable effect on the acoustic velocity of the liquid. This result confirmed that the slope of the V-shaped wave induced in under-liquid LSPs is determined by the ratio of the acoustic velocities in the solid and liquid media. Since this slope does not depend on laser pulse energy and can be measured directly and visually by imaging technique, we propose that the V-shaped wave can be used to investigate the acoustic properties of liquids.

3.2 Velocity of shock wave

We can see from the images (Fig. 1b) that the shock front traveled different distances in the four liquids after the same time interval. The images revealed that the fastest shock wave was induced in glycerol and the slowest shock wave was induced in silicone oil. To investigate the shock velocity, we followed the expansion of the shock fronts

induced in the liquids from 10 ns to microseconds after the irradiation.

During the early delay times (Fig. 1a), the black area on top of the target surface was the expanding shock wave followed by the high-pressure cavitation bubble [13]. We thus evaluated the shock front expansion by measuring the height of the black area and plotting it as a function of time. In Fig. 2, we present the time evolution of the height of the shock front induced in each liquid within 60 ns after irradiation. During this time interval, the expansion of shock fronts was not linear with the delay time. We, therefore, evaluated the change in shock velocity by dividing this time interval into two periods and estimating the shock velocity in each period by applying linear regression models to the data. The velocities of shock waves in the first period (20–40 ns) were estimated to be 4700 ± 600 m s^{-1} in glycerol, 3600 ± 300 m s^{-1} in water, 3500 ± 400 m s^{-1} in liquid paraffin, and 2800 ± 300 m s^{-1} in silicone oil. These velocities correspond to the Mach numbers $M \sim 2.4$ in glycerol, water, and liquid paraffin, and $M \sim 2.7$ in silicone oil. These high values of Mach number indicate that a strong shock was induced at the early delay time after the irradiation. In the second period (40–60 ns), the shock velocities reduced to 2400 ± 600 m s^{-1} in glycerol ($M \sim 1.3$), 2500 ± 600 m s^{-1} in water ($M \sim 1.7$), 2500 ± 500 m s^{-1} in liquid paraffin ($M \sim 1.8$), and 2100 ± 400 m s^{-1} in silicone oil ($M \sim 2$). These results show that the shock fronts expanded with sharply decreasing velocities in the liquids during the early time after irradiation.

After a few hundred of nanoseconds, the shock wave front detached from the cavitation bubble and displayed a good linear time-dependence. The shock velocities were estimated to be 2040 ± 30 m s^{-1} in glycerol, 1570 ± 50 m s^{-1} in liquid paraffin, and 1150 ± 30 m s^{-1} in silicone oil for the time interval from 400 to 1000 ns. These velocities correspond to the Mach number $M \sim 1.1$ in the

liquids, indicating weak shocks. This result is consistent with the behavior of shock wave observed in underwater LSP: The weak shock traveled at the velocity of 1550 ± 30 m s^{-1}, which was approximate 1.1 times higher than the acoustic velocity in water [13].

The phenomenon that the shock wave initially displays a nonlinear dependence behavior which progresses to a linear propagation has been reported for laser-induced shock wave in water [13, 19]. However, a detailed observation of the dynamical behavior of laser-induced shock process in organic liquids has not been reported in the literature. Our observation demonstrated that when the breakdown in the liquid phase was avoided, the shock wave induced in the organic liquids showed the same dynamical behavior with that induced in water: A strong shock was induced right after the laser shot, but rapidly transformed to a weak shock wave traveling at near the acoustic velocity. This transformation happens in only a few hundreds of nanoseconds after irradiation and should be taken into consideration when investigating the laser ablation of materials in organic liquids.

3.3 Strength of stress wave

In photoelastic images, the laser-induced stress wave (LSW) manifests itself as semicircles rapidly expanding into the solid target. The image of the stress wave in the solid phase includes a P-wave front followed by photoelastic fringes. The number of fringes shows the strength of LSW semiquantitatively: A larger number of fringes indicate a stronger stress [14]. Our observation showed a variance in the number of fringes, which is the indicative of the difference in the strength of LSW between the liquids. Figure 3 shows the number of fringes as a function of pulse energy, observed for each liquid at 1500 ns. At the same pulse energy, ablation in glycerol induced the largest number of fringes, which also means the strongest stress, while ablation in silicone oil induced the smallest number of fringes, which also means the weakest stress. Ablations in water and liquid paraffin showed an insignificant difference in the number of fringes, especially at small pulse energies. Over the investigated range of pulse energy, we found that the pulse energy required to induce a certain number of fringes can be reduced by an average of 20 % by using glycerol instead of water as the confining medium.

What makes the deviation in the strength of LSW induced in different liquids? We have measured the percentage of laser energy absorbed by each liquid when the laser beam is passed through a 5-mm liquid layer. The results indicated that the difference in lost energy is marginal between water, glycerol, liquid paraffin, and silicone oil under our experimental condition. The radiation absorption of liquid is, therefore, not seen as a reason for
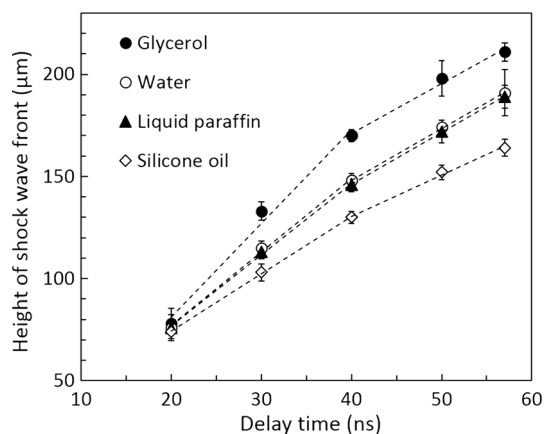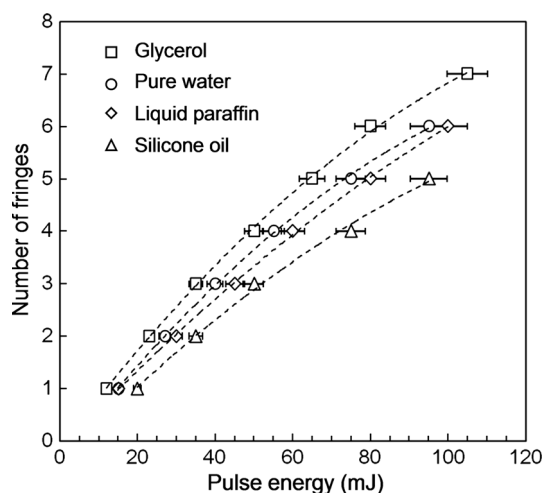
Fig. 2 Height of shock front as a function of time, observed for the shock processes induced in water, glycerol, liquid paraffin, and silicone oil. The pulse energy was 60 mJ. *Dashed lines* are best-fitting lines with linear regression models

Fig. 3 A comparison of the number of photoelastic fringes induced in water, glycerol, liquid paraffin, and silicone oil. The number of photoelastic fringes is observed at 1500 ns delay time and is plotted as a function of pulse energy for each liquid. The *error bars* show uncertainties in pulse energies, which is less than $\pm 5\%$

the difference in the strength of LSW induced in different liquids observed in our experiment. We also conducted the experiment to compare the ablation between silicone oils with different viscosities from 1 to 3000 cs and observed no dependence of the induced number of fringes on viscosity. We, therefore, rule out the possibility that the difference in the strength of the induced stress waves was due to the difference in viscosity of the four liquids.

For under-liquid laser-induced shock process, the plasma confinement effect and the impedance mismatch both contribute to the increase of shock pressure. The liquid phase acts as a restricting medium that restrains the plasma expansion, thereby inducing a much stronger shock. Zhang et al. [20] suggested that it is feasible to enhance the confining effect of the liquid overlay by increasing the density of the liquid. An analytical developed by Berthe et al. [21] predicted that the induced shock pressure P in LSP is proportional to the reduced shock impedance Z between the target material and the confining medium: $P \sim Z^{1/2}$. Thus, it is feasible to enhance the shock pressure

by selecting a confining medium with higher shock impedance. We, therefore, take the densities and shock impedances of the four liquids into consideration to explain the difference in the strength of LSW observed in our experiment. The shock impedance of each liquid was estimated as the product of the liquid density and the shock velocity measured in the time interval of 400 to 1000 ns. The reduced shock impedance Z between the target and a confining liquid was calculated by the equation: $2/Z = 1/Z_{target} + 1/Z_{liquid}$. The shock impedance of target was calculated as the product of its density and P-wave velocity measured in our experiment condition [13] and has the value of $Z_{target} = 0.325 \pm 0.016 \times 10^6$ g cm^{-2} s^{-1}. The results are presented in Table 1.

A consistent relationship between the liquid density and the strength of the induced stress waves was not observed in our experiment. Ablation in glycerol, which has the highest density, induced the strongest stress. Ablation in water resulted in a much stronger LSW in comparison with ablation in silicone oil, although the two liquids have approximately the same density. Liquid paraffin has the lowest density of the four liquids, but when being used as the confining medium, it induced a stress comparable to that induced in underwater ablation. In contrast, the relationship between shock impedance and the strength of LSW shows good consistency: Ablation in the liquid with a higher shock impedance resulted in a stronger stress. The effect of shock impedance on the strength of LSW can be explained by that the liquid which has a higher shock impedance will provide a better impedance matching with the target, and thus helps convert the shock energy into the mechanical impulse more efficiently.

The relationship between shock pressure P, reduced shock impedance Z, and laser intensity I can be expressed as $P \sim (Z)^{\frac{1}{2}}(I)^{\frac{1}{2}}$ [21]. The reduced shock impedance between the target and glycerol is 1.4 ± 0.1, 1.5 ± 0.1, and 1.7 ± 0.1 times higher than those between the target and water, liquid paraffin, and silicone oil, respectively. Thus, from the theoretical prediction, the laser intensity required to induce a certain value of shock pressure can be

Table 1 Characteristics of liquid overlays

	Glycerol	Water	Liquid paraffin	Silicone oil
Density ρ (g cm^{-3})	1.260	0.998	0.875 ± 0.015	0.970
Shock impedance[a] (10^6 g cm^{-2} s^{-1})	0.258 ± 0.004	0.153 ± 0.004	0.137 ± 0.004	0.112 ± 0.003
Reduced shock impedance[b] (10^6 g cm^{-2} s^{-1})	0.288 ± 0.015	0.208 ± 0.012	0.193 ± 0.011	0.167 ± 0.009

[a] Calculated from the density of the liquid ρ and shock velocity D measured in the time interval of 400–1000 ns: $Z_{liquid} = \rho D$

[b] Reduced shock impedance between the target and each liquid: $2/Z = 1/Z_{target} + 1/Z_{liquid}$

reduced by corresponding factors if we use glycerol as the liquid overlay instead of other liquids. We found from our experiment that using glycerol as the liquid overlay, the pulse energy required to induce the same number of fringes, that also mean the same level of shock pressure, was decreased by factors approximately 1.2 ± 0.1, 1.3 ± 0.1, and 1.5 ± 0.1 in comparison with ablations in water, liquid paraffin, and silicone oil, respectively. These values are lower than the values predicted by the theoretical model. At the laser intensity in GW range, the initial plasma is produced at the beginning of the laser pulse. During the rest of laser duration, the radiation is absorbed by the plasma through Inverse Bremsstrahlung mechanism. Unlike rigid confining medium which provides purely mechanical effects, the liquid phase contributes to the plasma formation process as well. The gasified materials induced in different liquids should have different properties that might also affect the induced pressure. Since our current observations cannot give any insight into the plasma and gasified material properties, we cannot fully explain the observed differences in the strength of stress wave induced in LSPs under different liquids. We propose that further studies on the effect of liquid properties on under-liquid LSP are needed. Nevertheless, our result still shows the feasibility of using a high-shock-impedance liquid to enhance the shock pressure induced in under-liquid LSP. For applications that require strong shock pressure like laser peening, we propose that high-shock-impedance liquid like glycerol can provide a better confining medium for LSPs.

4 Conclusions

The dynamical behaviors of laser-induced shock waves and stress waves in glycerol, liquid paraffin, and silicone oils were observed and compared to those induced in water. We showed that the shock impedance of the liquid caused a noticeable effect on the strength of laser-induced stress wave: Ablation in the liquid with a higher shock impedance resulted in a stronger stress. Among these liquids, ablation in glycerol induced the strongest stress and ablation in silicone oils induced the weakest stress. Compared to water, glycerol reduced the pulse energy required to induce a certain level of stress by about 20 %. Viscosity and the liquid density did not show a consistent relationship to the difference in the strength of stress wave observed in our experiment.

We also demonstrated that when the breakdown in the liquid phase was avoided, the laser-driven shock wave in all liquids showed the same dynamical behavior: A strong shock was induced right after the laser shot, but rapidly transformed to a weak shock wave traveling at approximate the acoustic velocity after a few hundreds of nanoseconds. The slope of the reflected wave in the inverted V-shape was shown to not depend on the laser pulse energy, but being determined by the ratio of the acoustic velocities in the solid and liquid media. We propose that the V-shaped wave can be employed to carry out the investigation into the acoustic properties of liquids.

References

1. A. Kruusing, Opt. Lasers Eng. **41**, 307 (2004)
2. A. De Giacomo, M. Dell'Aglio, A. Santagata, R. Gaudiuso, O. De Pascale, P. Wagener, G.C. Messina, G. Compagnini, S. Barcikowski, Phys. Chem. Chem. Phys. **15**, 3083 (2013)
3. R.K. Thareja, S. Shukla, Appl. Surf. Sci. **253**, 8889 (2007)
4. A. Nath, A. Khare, J. Appl. Phys. **110**, 043111 (2011)
5. W.T. Nichols, T. Sasaki, N. Koshizaki, J. Appl. Phys. **100**, 114913 (2006)
6. G. Yang, Prog. Mater Sci. **52**, 648 (2007)
7. V. Amendola, S. Polizzi, M. Meneghetti, J. Phys. Chem. B **110**, 7232 (2006)
8. V. Amendola, S. Polizzi, M. Meneghetti, Langmuir **23**, 6766 (2007)
9. V.S. Burakov, A.V. Butsen, N.V. Tarasenko, J. Appl. Spectrosc. **77**, 386 (2010)
10. S.M. O'Malley, B. Zinderman, J. Schoeffling, R. Jimenez, J.J. Naddeo, D.M. Bubb, Chem. Phys. Lett. **615**, 30 (2014)
11. T. Kovalchuk, G. Toker, V. Bulatov, I. Schechter, Chem. Phys. Lett. **500**, 242 (2010)
12. T.T.P. Nguyen, R. Tanabe, Y. Ito, Appl. Phys. Express **6**, 122701 (2013)
13. T.T.P. Nguyen, R. Tanabe, Y. Ito, Appl. Phys. A **116**, 1109 (2013)
14. T.T.P. Nguyen, R. Tanabe, Y. Ito, Appl. Phys. Lett. **102**, 124103 (2013)
15. L. Martí-López, R. Ocaña, J.A. Porro, M. Morales, J.L. Ocaña, Appl. Opt. **48**, 3671 (2009)
16. J. Lubbers, R. Graaff, Ultrasound Med. Biol. **24**, 1065 (1998)
17. W. Benenson, J.W. Harris, H. Stocker, H. Lutz (eds.), *Handbook of Physics* (Springer, New York, 2002)
18. Shin-Etsu chemical Co., Ltd, KF-96 Performance Test Result. http://www.silicone.jp/e/catalog/pdf/kf96_e.pdf
19. B.D. Strycker, M.M. Springer, A.J. Traverso, A.A. Kolomenskii, G.W. Kattawar, A.V. Sokolov, Opt. Express **21**, 23772 (2013)
20. Y. Zhang, Y. Gu, X. Zhang, J. Shi, J. Zhou, J. Appl. Phys. **100**, 103517 (2006)
21. L. Berthe, R. Fabbro, P. Peyre, L. Tollier, E. Bartnicki, J. Appl. Phys. **82**, 2826 (1997)